

Capacitance of a molecular overlayer on the silicon surface measured by scanning tunneling microscopy

Ryota Akiyama, Takuya Matsumoto,* and Tomoji Kawai

The Institute of Scientific and Industrial Research, Osaka University, 8-1 Mihogaoka, Ibaraki, Osaka 567-0047, Japan

(Received 3 January 2000; revised manuscript received 11 February 2000)

The capacitance of ultrathin cyclopentene overlayers on a Si(100)- 2×1 surface have been measured using scanning tunneling microscopy (STM). Both tunneling barrier height spectroscopy and tunneling barrier height imaging were used to obtain the values of tip-surface separation, electric field, and the apparent tunneling barrier height of the surface. The apparent tunneling barrier height indicates the magnitude of a local electronic charge on the surface, which corresponds to the capacitance of molecular overlayer. In this study, the capacitance of single molecule adsorption area was found to be $C=1.3\times 10^{-20}$ F, which comprises the dipole moment of cyclopentene molecule itself and the charge transfer between the molecule and the surface. A series of STM measurements for determining the capacitance of nanometer-scale structures was then proposed.

I. INTRODUCTION

Given the current rapid development of microfabrication and passivation techniques, electronic devices fabricated on silicon wafers have become progressively smaller. Lithographic techniques permit the fabrication of nanometer structures on the order of 10 nm in plane. Silicon oxide has served as the main passivation route for the insulation layer down to thickness of 0.1 nm, and some other nonoxidized atomic-scale materials have also been fabricated on silicon wafers.¹ As these electronic devices are reduced to a nanometer scale, several mesoscopic quantum effects appear. One of the latest topics is quantized conductance in nanoconducting wire, such as carbon nanotubes which restrict the conductance according to $G=1/R=h/4e^2$, based on Pauli's principles.² Much attention is also being directed toward single-electron tunneling in extremely small double-tunneling junctions (e.g., single-electron transistors), which were satisfied with the capacitance of $C<0.1e^2/k_B T$ and resistance of $R>h/e^2$.³ These requirements show that the ability to control the functioning and characteristics of these nanometer-scale devices on the silicon wafers in terms of resistance R and capacitance C would be highly significant. However, in this scale range, the geometric configuration of the device is no longer helpful for estimating R and C , as the surface/interface characteristics have an increasing influence on the functioning of the device. For this reason, an analytical method is required to characterize the nanometer-scale devices on the silicon surfaces.

This paper describes how the authors evaluated the capacitance of a single molecular overlayer using scanning tunneling microscopy (STM). STM has advantages over various other useful methods of surface analysis for studying local electronic states within a few eV from the Fermi level. Scanning tunneling spectroscopy (STS) provides surface densities of states, which can arise from the surface-projected bulk band structure or from a true surface state. Furthermore, tunneling barrier height spectroscopy and tunneling barrier height imaging, which are derivative techniques of STM and STS, are capable of measuring the apparent tunneling

barrier height between the tip and surface. The apparent tunneling barrier height can be useful to detect the local electronic charge on the surface, which involves chemical identification, band-bending effects, and surface capacitance.

The experiments were performed on an ultrathin cyclopentene overlayer formed on a Si(100)- 2×1 surface.⁴ Cyclopentene molecules were adsorbed on 2×1 dimer rows by breaking the π bonds (C=C) of cyclopentene and the Si dimers (Si=Si), and bonding to the surface via the two newly formed σ bonds (Si-C) by 2+2 cycloaddition. By using this type of chemically tailoring system, a wide variety of characteristics can be synthesized and incorporated on a silicon surface of very thin and highly uniform thickness.¹

II. METHOD

The experiments were carried out using UHV-STM (approximately 8.0×10^{-11} Torr) at room temperature. The tip was mechanically polished Pt/Ir wire which was polycrystalline and 0.5 mm diameter. The substrate was a phosphorous-doped (0.01–0.1 Ω cm) n -type Si(100) wafer. It was annealed for 10 h at 650 $^\circ$ C for outgassing, and a clean 2×1 surface was prepared by flash-heating up to 1200 $^\circ$ C for 10 sec. The cyclopentene molecules were purchased from Aldrich with a minimum purity of 97%. The Si(100) was exposed to the 1.0×10^{-8} Torr cyclopentene molecules for 2 min in the UHV chamber.

In this study, the three different kinds of measurement were used: STS, tunneling barrier height spectroscopy (BHS), and tunneling barrier height imaging (BHI). In a simple one-dimensional model, the tunneling current in STM can be expressed as

$$I_t = \int_{E_F}^{E_F+V_s} \rho_{\text{sur}} \exp(-1.025\sqrt{\phi_{\text{app}}z}) dE, \quad (1)$$

where I_t and V_s are the tunneling current and voltage, respectively, ρ_{sur} is the surface local density of state, ϕ_{app} is the average barrier height in eV, and z is the tip-surface separation in \AA units. In STS measurements, the differential conductance dI_t/dV_s qualitatively reflects the surface den-

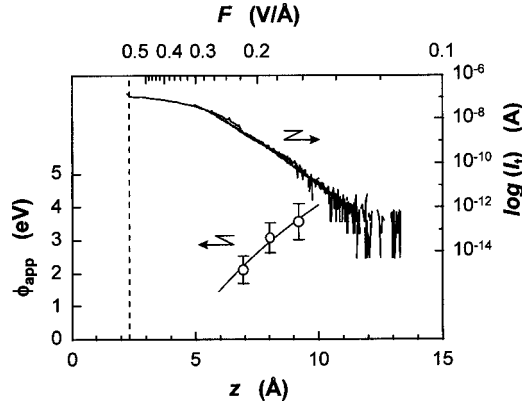


FIG. 1. The upper results (right ordinate) show typical experimental data for the tunneling current $\ln(I_t)$ against tip-sample separation z on the Si(100)- 2×1 surface taken at $V_s = -1.5$ V. The steep current surge at $z = 2.34$ Å (dashed line) corresponds to an electrical contact between the tip and surface. The lower results (left ordinate) show the plots of ϕ_{app} against the tip-sample separation z which were given by gradients of numerous $\ln(I_t)$ - z samples at $V_s = -1.5$ V.

sity of states $\rho_{\text{sur}} \approx dI/dV_s$.⁵ The apparent tunneling barrier height ϕ_{app} can be also obtained from Eq. (1) as follows:⁵⁻⁷

$$\phi_{\text{app}} = \left[\frac{1}{1.025} \frac{d \ln(I_t)}{dz} \right]^2. \quad (2)$$

As an experimental procedure, BHI imaging was performed using a lock-in technique by modulations $\Delta z = 1$ Å and $f = 4$ kHz. Schuster *et al.* reported that an internal inconsistency between the values obtained from the corrugation at different tunneling currents and the values measured by a lock-in technique could not be resolved.⁸ This means that the lock-in technique often provides anomalous ϕ_{app} values, especially on highly corrugated surface. For this reason, we also measured BHS to calibrate the absolute values of the apparent barrier height in BHI. As Olsen *et al.* demonstrated, measurements of individual $\ln(I_t)$ - z curves did not reveal anomalously low values.^{6,7} In the actual measurement of $\ln(I_t)$ - z , the dynamic range of the current amplifier was limited when scanning the tip along the z direction over the full tip-displacement range. For this reason, the values of $I(\Delta z)$ were measured as a partial data series obtained at different feedback positions with displacement Δz of ± 3 Å. The overall characteristics were then compiled based on these results. All $\ln(I_t)$ - z measurements were performed during an open feedback loop for 1.3 sec.

III. RESULTS AND DISCUSSION

Initially, our aim was to measure tip-sample separation z , electric field $F = V_s/z$, and apparent tunneling barrier height ϕ_{app} on a clean Si(100)- 2×1 surface, which are the basic parameters required to determine the capacitance of the ultrathin cyclopentene overlayer. All of these parameters can be obtained by $\ln(I_t)$ - z curve measurement in BHS: total displacement from the feedback position to current jump in the curve gives absolute z and $F = V_s/z$, and the gradient of the $\ln(I_t)$ - z curve provides the value of ϕ_{app} according to Eq. (2).

The upper plots in Fig. 1 indicate a typical $\ln(I_t)$ - z curve

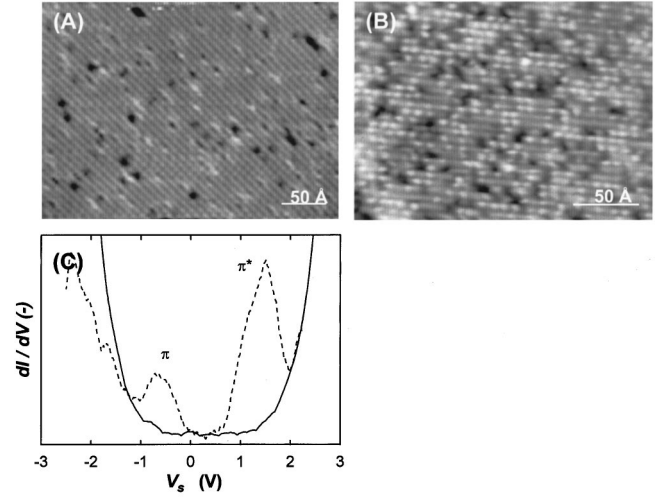


FIG. 2. Filled-state STM images of (A) a clean Si(100)- 2×1 surface and (B) Si(100)- 2×1 surface after exposure to 1.8-L cyclopentene at room temperature. The cyclopentene molecules were adsorbed twice on the 2×1 unit cell of the Si(100) surface. (C) The results for dI_t/dV_s on a clean Si(100)- 2×1 surface (dashed line) and an ultrathin cyclopentene overlayer (solid line). The π and π^* states of the Si(100)- 2×1 surface are eliminated by cyclopentene adsorption, and a wide energy gap arises.

on the Si(100)- 2×1 surface with $V_s = -1.5$ V. (The dashed line corresponds to the position of the surface.) A steep “current jump” in the $\ln(I_t)$ - z curve indicates the transition from vacuum electron tunneling to conductive current, corresponding to the interatomic contact of two Si atoms at $z = 2.3$ Å. Absolute z and $F = V_s/z$ values, that are shown in the lower and upper scales in Fig. 1, can be calibrated from this electrical contact.⁹ As the tip approaches the surface, the derivative of $\ln(I_t)$ - z saturates gradually until electrical contact occurs. This saturation corresponds to the reduction of ϕ_{app} , as expressed in Eq. (2). The reduction of ϕ_{app} in the metal-insulator-semiconductor junction has already been predicted theoretically due to the band-bending effect.¹⁰ Chen and Hamers observed a steep increase of ϕ_{app} at $z \leq \sim 1.5$ Å on a Si(111) surface, due to the effect of dynamic tip-atom relaxation.¹¹ However, we did not observe this phenomenon on a Si(100)- 2×1 surface. The values of ϕ_{app} in the lower data of Fig. 1 were calculated by Eq. (2) using the $\ln(I_t)$ - z relationship obtained above. At a large separation, ϕ_{app} should approach $\phi_{\text{Si}} = 5.6$ eV at $V_s = -1.5$ V ($\phi_{\text{Si}} = 4.1$ eV at $V_s = +1.5$ V), which is the average barrier height for a square barrier.^{12,13}

As a next step, we measured dI_t/dV_s curves for both the bare Si(100)- 2×1 surface and the ultrathin cyclopentene overlayer. Figure 2 (A) shows a STM image of atomically flat terraces and Si dimer rows of a Si(100)- 2×1 surface observed in a filled state. The dimers are separated by a surface lattice constant of $a_0 = 3.84$ Å within each row, while the rows are separated by $2a_0 = 7.7$ Å, resulting in a 2×1 periodicity. Figure 2(B) shows a STM image of Si(100)- 2×1 after exposure to 1.8 L of cyclopentene at room temperature. The cyclopentene molecules appear as round and bright protrusions ordered in rows, with the spacing between molecules typically being twice the space of 3.84 Å which separates the Si=Si dimers. As Chen and Hamers reported, the

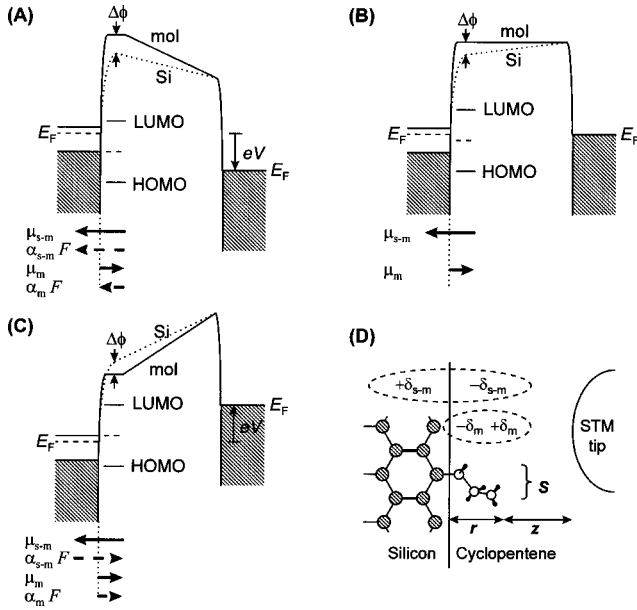


FIG. 3. Energy diagram for determining the charge transfer between the molecule and the substrate. (D) A total dipole moment μ_{total} at the molecule site consists of four components: the permanent dipole moment μ_m and induced dipole moments $\alpha_m F$ of the molecule itself, the charge transfer between the substrate and molecule due to adsorption μ_{s-m} , and the external field $\alpha_{s-m} F$. The dipole moments are represented by arrows from negative charge to positive charge (B) Even with zero bias voltage, a surface electric dipole moment μ_{s-m} and μ_m is formed by molecule adsorption. Electric dipole moments $\alpha_{s-m} F$ and $\alpha_m F$ should also be induced by a negative (A) or a positive (C) external field. The surface dipole moment forms an electric potential, which changes the effective apparent barrier height $\Delta\phi_{app}$ for electron tunneling.

cyclopentene molecules are located on dimer rows by breaking the cyclopentene (C=C) π bonds, and the Si dimers (Si=Si) are then bonded to the surface by forming two new σ bonds (Si—C).⁴ Therefore, this molecular overlayer is very thin and uniform with a molecular-size unit. In Fig. 2(C), the relationship dI_t/dV_s , as a function of V_s on an ultrathin cyclopentene overlayer (solid line), is shown together with that of an Si(100)-2 \times 1 clean surface (dashed line). The Si(100)-2 \times 1 spectrum shows a π occupied state at -0.6 eV, and a π^* unoccupied state at 1.5 eV with an energy gap of $E_g \sim 0.8$ eV.¹⁴ In contrast, the spectrum for ultrathin cyclopentene overlayer shows a wide energy gap of $E_g \sim 1.8$ eV, with no surface states. This result shows that chemically reactive adsorption forming σ bonds (Si—C) extinguishes the π states of dangling bonds. This elimination of silicon surface states means that the cyclopentene monolayer is functioning as an ultrathin insulator layer, which might be useful to constitute a quantum well along the normal direction to the surface.

Finally, the capacitance of the ultrathin cyclopentene overlayer is estimated below. Generally, a dielectric constant depends on the nature of the material itself: the polarization of electron clouds, atoms, and dipoles. However, if the thickness of the overlayer is reduced to molecular size, the interaction between the overlayer and substrate would become more significant than its bulk property. In particular, the charge transfer between the molecular overlayer and sub-

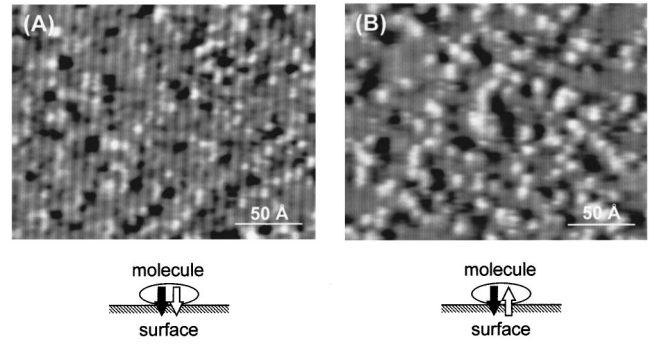


FIG. 4. Tunneling barrier-height images of cyclopentene molecules adsorbed on the Si(100)-2 \times 1 surface at (A) $V_s = -1.5$ V and (B) $V_s = +1.5$ V. The brighter points represent higher tunneling barrier heights. In these observations, the molecules are always rendered brightly, indicating that the barrier height is enhanced by the presence of cyclopentene molecules. Though some C defects on the Si(100)-2 \times 1 surface were also imaged brightly at $V_s = +1.5$ V, they could be distinguished from cyclopentene by their size. The insets show the dipole directions by molecule adsorption $\mu_m + \mu_{s-m}$ (black arrow) and an external field $(\alpha_m + \alpha_{s-m})F$ (white arrow).

strate affects the effective capacitance of the overlayer. Figures 3(A)–3(D) show the influence of dipole moments on the tunneling barrier between the tip and the silicon substrate. A total dipole moment μ_{total} at the molecule site consists of four components: the permanent dipole μ_m and the induced dipole moments $\alpha_m F$ of the molecule itself, and the charge transfer between the substrate and molecule due to adsorption μ_{s-m} and external field $\alpha_{s-m} F$. Here, $\alpha_{m,s-m}$ is the polarizability, and F is an external field. These four dipole moments are represented by arrows from negative charge to positive charges in Fig. 3, whose directions correspond to our experimental results. The molecule-substrate charge transfer owing to molecule adsorption μ_{s-m} is induced by the difference between the substrate work function ϕ_s (dashed line at substrate) and the molecule's chemical potential (the dashed line at the molecule). As a result, a molecular charge $-\delta_{s-m}$ and an opposite substrate charge $+\delta_{s-m}$ arise at the interface [Fig. 3(D)]. For a low bias voltage, dipole moments μ_{s-m} and μ_m form an electric potential, which changes the effective apparent barrier height for electron tunneling [Fig. 3(B)]. Conversely, electric dipole moments $\alpha_m F$ and $\alpha_{s-m} F$ are also induced in the presence of an external field, as shown in Figs. 3(A) and 3(C). An external field shifts the position of molecule's chemical potential (dashed line at the molecule). This charge transfers $\alpha_m F$ and $\alpha_{s-m} F$ can be reversed by changing the direction of the external field, whereas the directions of μ_m and μ_{s-m} are not concerned with the external field but determined by the nature of molecular adsorption. Accordingly, the magnitude of total dipole moment μ_{total} can be estimated by measuring the tunneling barrier-height images. This can be expressed as

$$\mu_{total} = (\mu_m + \mu_{s-m}) + (\alpha_m + \alpha_{s-m})F = \Delta\phi_{app} \left(\frac{\epsilon_0 S}{e} \right), \quad (3)$$

where $\Delta\phi_{app}$ is the difference in the apparent tunneling barrier height between the clean surface and the

TABLE I. Results and parameters for calculating the capacitance, the induced dipole, and the permanent dipole of an ultrathin cyclopentene overlayer $I_t = 10$ PA, $r = 5.0$ Å, and $S = 57.8 \times 10^{-20}$ m².

	$V_s = 1.5/-1.5$ (V)				$\mu_{s-m} + \mu_m$ (C m)	$\alpha_{s-m} + \alpha_m$ (Cm ² /V)	C_{mol} (F)
	z (Å)	F (V/Å)	ϕ_{app} (eV)	$\Delta\phi_{\text{app}}$ (eV)			
Si(100)-2×1 surface	8.9/9.3	0.17/-0.16	2.92/3.08				
Ultrathin cyclopentene overlayer	9.4/9.8	0.16/-0.15	3.07/3.42	0.15/0.34	-1.24×10^{-30}	0.66×10^{-39}	1.3×10^{-20}

adsorbate-adsorbed surface, F is electric field, S and ϵ_0 are the molecule adsorption area and the permittivity in free space, respectively.^{9,15} This expression implies that the tunneling electrons encounter a higher or lower barrier height than that of the clean surface when the electrons pass through an adsorbed molecule with an upward or downward dipole moment on the surfaces. Here, the capacitance of single molecule adsorption area C_{mol} can be expressed as

$$C_{\text{mol}} = \frac{\epsilon_r \epsilon_0 S}{r} = \left(1 + \frac{N(\alpha_{s-m} + \alpha_m)}{\epsilon_0} \right) \frac{\epsilon_0 S}{r}, \quad (4)$$

where N is the number of molecules contained in a unit (m^{-3}), and r is the thickness of the molecular overlayer.

Figures 4(A) and 4(B) show tunneling barrier-height images of cyclopentene molecules adsorbed on the Si(100)-2×1 surface at (A) $V_s = -1.5$ V and (B) $V_s = +1.5$ V. The brighter points in the gray scale represent the higher tunneling barrier heights. In the observation at $V_s = -1.5$ V, the molecules are rendered as small and bright spots, indicating that the barrier height is enhanced by the presence of cyclopentene molecules. Conversely, we have observed two types of protrusions at $V_s = +1.5$ V, specifically extremely large spots and small spots. We have confirmed that the large spots were C defects on the Si(100)-2×1 surface, and the small spots were cyclopentene molecules, which were distinguishable by their sizes.¹⁶ In these observations, the molecules are always rendered brightly at both bias polarities. A high barrier height at the molecule site implies that the total dipole moment μ is always directed from the vacuum to the surface, despite the polarity change. The value of $\Delta\phi_{\text{app}}$ however, changes with the values of z and F . In fact, the values of $\Delta\phi_{\text{app}}$ are 0.15 eV at $V_s = -1.5$ V and 0.34 eV at $V_s = +1.5$ V. This variation is attributed to the contribution of an induced dipole, for which the orientation is inverted by the polarity change of F .⁹

Here the authors have calculated the dipole moment $\mu_m + \mu_{s-m}$, $(\alpha_m + \alpha_{s-m})F$ and the capacitance of single molecule adsorption area C_{mol} by solving two simultaneous equations:

Eq. (3) with $V_s = \pm 1.5$ V. The values used for the calculation are contained in Table I. The value of S was obtained from the STM images; $S = 57.8 \times 10^{-20}$ m² for the molecule adsorption area corresponded to twice the 2×1 unit cell of the Si(100) surface. The value of r is determined by structure model, as shown in Fig. 3(D), where we used a van der Waals adsorption height $r = 5.0$ Å for cyclopentene molecule. The results are $\mu_{s-m} + \mu_m = -1.24 \times 10^{-30}$ C m (0.37 D), and $\alpha_{s-m} + \alpha_m = 0.66 \times 10^{-39}$ Cm²/V. Since the molecular calculations (PC-SPARTAN, ©1996 by Wavefunction, Inc) yield $\mu_m = -5.00 \times 10^{-31}$ C m (0.15 D) for isolated cyclopentene molecules, $\mu_{s-m} = -7.4 \times 10^{-3}$ C m (0.22 D) is attributed to a charge transfer between the cyclopentene molecule and the silicon substrate. Assuming an adsorption distance 3.5 Å between the cyclopentene molecule and silicon substrate, a cyclopentene molecule would always have a negative charge for $\delta = -0.013e$. Furthermore, we have also calculated the relative dielectric constant for the ultrathin molecule overlayer to be $\epsilon_r = \{1 + N(\alpha_{s-m} + \alpha_m)/\epsilon_0\} = 1.26$, which is about half of magnitude compared with benzene molecule ($\epsilon_r = 2.3$) and cyclohexane molecule ($\epsilon_r = 2.0$) in the liquid phase. These results suggest that the field-induced polarization is suppressed for an ultrathin molecular overlayer. Finally, the capacitance of single molecule adsorption area is calculated for $C_{\text{mol}} = 1.3 \times 10^{-20}$ F.

IV. CONCLUSION

In conclusion, we have attempted to use STM in order to evaluate the capacitance of nanometer-thickness organic overlayers. Measured values of dI_t/dV_s yield the conductivity of the ultrathin molecule overlayer, while BHS and BHI provide the values of ϕ_{app} , z , and F , which can be used to obtain the capacitance of the ultrathin molecule overlayer. When the thickness of the overlayer is reduced to nanometer scale, the capacitance become smaller than that of organic materials. We believe that these measurements are useful for evaluating the surface conductivity and capacitance of nanometer-scale devices formed on a silicon surface.

*Fax: 81-6-6875-2440. Email: matsumoto@sanken.osaka-u.ac.jp

¹J. M. Buriak, Chem. Commun. (Cambridge), 1051 (1999).

²M. Bockrath, D. H. Cobden, J. Lu, A. G. Rinzler, R. E. Smalley, L. Balents, and P. L. McEuen, Nature (London) **397**, 598 (1999).

³Single Charge Tunneling: Coulomb Blockade Phenomena in Nanostructures, Vol. 294 of NATO Advanced Study Institute Series B: Physics, edited by H. Grabert and M. H. Devoret (Plenum, New York, 1993).

num, New York, 1993).

⁴J. S. Hovis, H. Liu, and R. J. Hamers, Surf. Sci. **402**, 1 (1998); J. Vac. Sci. Technol. B **15**, 1153 (1997); Appl. Phys. A: Mater. Sci. Process. **66**, S553 (1998).

⁵Scanning Tunneling Microscopy and Spectroscopy: Theory, Techniques, and Applications, edited by D. A. Bonnelli (VCH, New York, 1993).

⁶L. Olesen, M. Brandbyge, M. R. Sorensen, K. W. Jacobsen, E.

- Lagsgaard, and F. Besenbacher, Phys. Rev. Lett. **76**, 1485 (1996).
- ⁷L. Olesen, E. Lagsgaard, I. Stensgaard, and F. Besenbacher, Appl. Phys. A: Mater. Sci. Process. **66**, S157 (1998).
- ⁸R. Schuster, J. V. Barth, J. Winterlin, R. J. Behm and G. Ertl, Ultramicroscopy **42-44**, 533 (1992).
- ⁹R. Akiyama, T. Matsumoto, and T. Kawai, J. Phys. Chem. B **103**, 6103 (1999); Surf. Sci. Lett. **418**, L73 (1998).
- ¹⁰M. Weimer, J. Kramer, and J. D. Baldeschwieler, Phys. Rev. B **39**, 5572 (1989).
- ¹¹C. J. Chen and R. J. Hamers, J. Vac. Sci. Technol. B **9**, 503 (1991).
- ¹²J. G. Simmons, J. Appl. Phys. **34**, 1793 (1963); **34**, 2581 (1963).
- ¹³After $\Delta\phi_{\text{Si}}=4.3$ eV and $\Delta\phi_{\text{Pt}}=5.4$ eV were assumed for *n*-Si(100) and a platinum tip, respectively, the apparent barrier for a square barrier was determined to be $\phi_{\text{Si}}=4.1$ eV ($V_s=+1.5$ V) and $\phi_{\text{Si}}=5.6$ eV ($V_s=-1.5$ V).
- ¹⁴M. McEllistrem, G. Haase, D. Chen, and R. J. Hamers, Phys. Rev. Lett. **70**, 2471 (1993).
- ¹⁵J. K. Spong, Nature (London) **338**, 137 (1989).
- ¹⁶R. J. Hamers and U. K. Kohler, J. Vac. Sci. Technol. A **7**, 2854 (1989).